An Inertial Sensor System for Measurements of Tibia Angle with Applications to Knee Valgus/Varus Detection

Wenzheng Hu [#1], Edgar Charry [#2], Muhammad Umer [#3], Andrew Ronchi [#4], Simon Taylor [*5]

[#] *dorsaVi Pty Ltd*
Level 1, 120 Jolimont Road, Melbourne, Australia
[1] vincent@dorsavi.com
[2] echarry@dorsavi.com
[3] mumer@dorsavi.com
[4] ar@dorsavi.com

[*] *Victoria University - School of Sport and Exercise Science (SES)*
Room L122, Level 1, Building L, Ballarat Road, Footscray, Melbourne, Australia
[5] simon.taylor@vu.edu.au

***Abstract*—Accurate measurement of knee motion during dynamic movements is the key to detect and highlight deficiencies in peripheral muscles and ligaments of the knee and hence to predict the risk of injury. Miniature inertial sensors are increasingly becoming a viable option for human movement measurement, given their small size, low cost and relatively good accuracy compared with traditional optical measurements. A system capable of measuring tibia angle using a shank mounted wireless inertial sensor is proposed. The system employs a simple setup with only one skin-mounted triaxial accelerometer and gyroscope module attached to the tibia segment, and an algorithm to estimate the tibia angle. The accuracy of the system was assessed by an optical tracking system (Optotrak Certus) during dynamic movements performed by three subjects by evaluating Root-Mean-Square Error (RMSE) of tibia-flexion and tibia-adduction angles over the period of motion. We achieve an RMSE of 1.6 ± 1.1 and2.5 ± 1.6 degrees in tibia-flexion and tibia-adduction angles, respectively. It is argued that tibia angle can be reliably used to detect valgus or varus movement of the knee and hence the proposed system provides a simple and useful assessment tool for performance enhancement and rehabilitation.**

I. Introduction

Lower limb injuries account for a significant proportion of injuries in high performance sports [1] and inflict a high cost on health care systems around the world. For instance, lower limb injuries cost an estimated 2.5 billion annually to the health-care system in the United States [2]. Knee injuries are not only the most common, but they also have the most serious consequences, such as Patellar Tendinopathy (Jumper's Knee), Patellofemoral Syndrome or Anterior Cruciate Ligament (ACL) Injury [3].

Knee abduction (or knee valgus) has been shown to be a predictive factor of ACL injury in athletes and therefore its detection has great relevance in the clinical setting [4]. Assessment of knee injury risk is usually based on qualitative observation of knee motion during single-legged weight-bearing tasks (e.g. hopping) [5]. However, clinicians cannot reliably detect at-risk knee positions by the naked eye. Traditionally, if clinicians had wanted to accurately quantify knee kinematics, they would have commonly used a motion capture system [6] [7]. However, it is difficult to replicate tasks of the sports-field environment in the constraints of the lab-environment, where motion capture systems are operated from. As an effective alternative, small light-wearable body sensors offer a user-friendly solution because they minimise most of the constraints that are associated with a motion capture system.

In related literature, Cooper et al. [8] developed a Kalman-filter based gait knee angle estimation using accelerometers and gyroscopes. Sensor units were attached on the shank and thigh. Although the reported Root Mean Square Error (RMSE) of the measurements in knee flexion angle during walking was 3.4° with 1.1° standard deviation, the skin motion artifact of the thigh affected adversely the overall results. Kawano et al. [9] presented an analysis on **3D** knee angles when squatting using accelerometers, gyroscopes and magnetometers. The reported error was 0.7 ± 6.9 degrees in knee flexion. However, the unreliability of magnetic field in real environment, ongoing magnetization within the magnetometer and continuous presence of magnetic disturbances resulted in negative effects on the accuracy of such a system. Dejnabadi et al. [10] reported a system that measured **2D** knee joint angles using body mounted accelerometers and gyroscopes. The result showed low error (1.3°) and high correlation ($R = 0.997$) of sagittal plane angle compared to an ultra-sound motion measurement system. However, their method could only estimate knee kinematics in one dimension.

In this paper, we propose an inertial sensor system that can be used for detection and measurement of valgus or varus motion of the knee based on angular motion of the tibia. While tibia motion alone does not completely describe the knee, it can also be acknowledged that accurate motion capture systems will always have trouble accurately measuring the thigh because skin-mounted-markers do not completely describe the state of the underlying thigh (femur) bone. Tracking the motion of the tibia is not subjected to these problems. Therefore, motion of the tibia is more likely to contain uncorrupted details

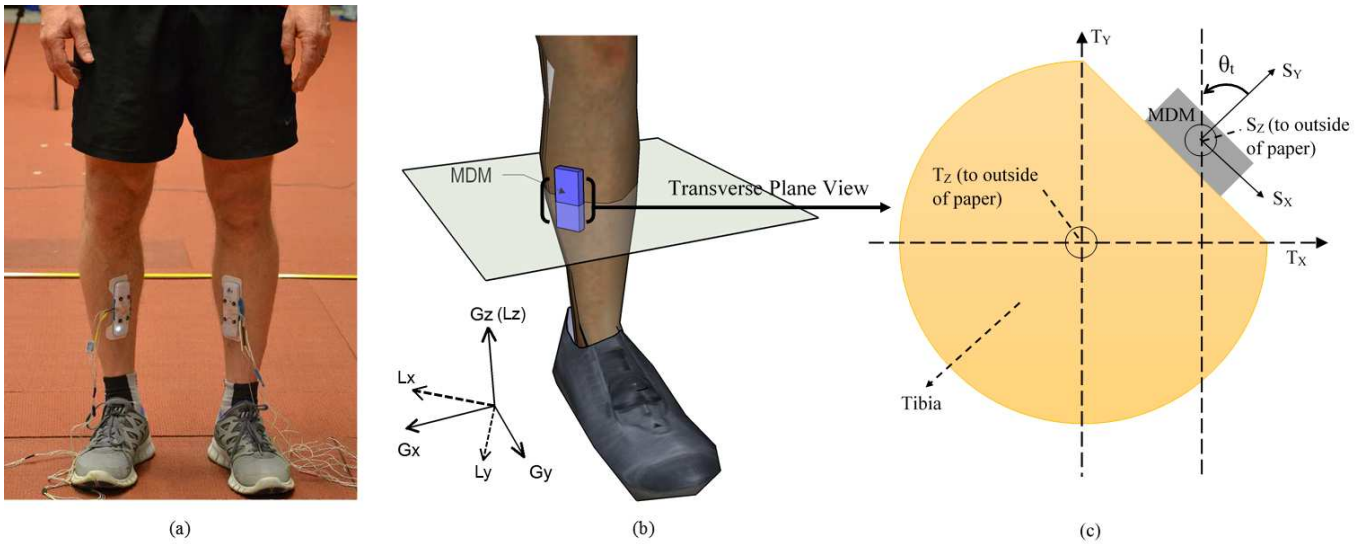

Fig. 1. Sensor placement from different view. (a) Two sensor units placed on left and right tibia of subject 1 (coronal plane view). (b) Sensor unit placed on left leg, showing lab-CS and global-CS. (c) Transversal plane view of sensor placement on the left leg, showing sensor-CS, tibia-CS and the angle θ_t.

of the state of the knee. We argue that if tibia motion can be accurately measured from an inertial sensor, then clinicians will have a viable solution for assessing knee injury risk. This is investigated by using a sensor placed on the anterior surface of the tibia, which has been proven a reliable landmark in previous studies [11]. In addition, while most of studies have focused on single-leg squats or gait [12] [13], we also report measurements for highly dynamic motion, i.e. single-leg hops. We validated our system against a *gold standard* optical motion capture system, namely the Optotrak Certus.

The rest of paper is arranged as follows: Section II describes the hardware, methodology of experiments and the data processing flow; Section III and IV report on experimental results and provide a comprehensive discussion, respectively; Conclusions are summarized in section V.

II. Experimental Methodology

A. Hardware and Placement

1) Sensor Unit: The hardware used in the system, namely the 'Measurement Device - Movement' (**MDM**) [14], employs one low-power triaxial accelerometer with magnetometer (ST Microelectronics $LSM303DLHC$ [15]) and one triaxial gyroscope (ST $L3G4200D$ [16]). Data from the sensors were sampled at 200Hz on all three axes and sent through a serial interface to the micro-controller. Full scale inputs to accelerometer and gyroscope are $\pm 24g$ and ± 250 degrees per second, respectively. Sensor readings are transmitted through wireless channel to a recording and feedback device, from which data can be offloaded onto PC for further analysis.

2) Reference System: The reference system used in this experiment was NDI Optotrak Certus [17]. The system has a **3D** resolution of 0.01mm and maximum marker rate of 3500Hz. Four NDI infra-red emitting tracking markers were attached to each sensor unit($S_X S_Z$ in Figure 1). The position of the NDI tracking markers was collected using NDI's First-Principles software [18]. The camera capture rate was set at 300Hz, but this was subsequently down-sampled to 200Hz during post-processing to match the sensor data sampling rate.

3) Sensor Placement: In this application, the sensor unit is placed along anterior surface of the tibia along the longitudinal axis, the mid-point between the knee and the ankle. The placement of sensor units and Optotrak markers are depicted in Figure 1(a).

4) Measurement coordinate systems (CS): Figure 1(b) and (c) defines the following CS: the global-CS $\mathbf{G}$ (G_X, G_Y, G_Z), the lab-CS $\mathbf{L}$ (L_X, L_Y, L_Z), the sensor-CS $\mathbf{S}$ (S_X, S_Y, S_Z) and the tibia-CS $\mathbf{T}$ (T_X, T_Y, T_Z). Planes XY, YZ and ZX correspond to transverse, sagittal and frontal planes respectively. The sensor unit is carefully placed so that the S_Z axis is approximately in line with T_Z axis. Angle θ_t is defined as the rotation angle from S_Y axis to T_Y axis. The tibia-flexion, tibia-adduction and tibia-twist angles are defined as angular displacements occurring about G_X, G_Y and G_Z respectively. These angles are derived from the convention of three-dimensional Euler transformation of the tibia orientation. Positive tibia-adduction angle (i.e. proximal end of the tibia tilts lateral) is associated with knee adduction/varus and negative tibia-adduction angle (i.e. proximal end of tibia tilts medial) is associated with knee abduction/valgus. The frontal plane projection angle (FPPA) is the angular displacement of the tibia based upon the projection of the tibia segment (T_Z) onto the global frontal plane (G_Z).

B. Test Protocol

Three healthy male subjects with no lower limb disorders participated in the experiment. Subjects were instructed to perform two types of movement tasks, single-leg squats and single-leg hops. The squat task hold > 2 seconds. Three types of squat and hop tasks were assigned, each with simulated normal, outwards (varus) and inwards deviation (valgus) of the knee. Each type of squat and hop was repeated 3 times. Data was collected simultaneously from the sensor and the Optotrak system. All experiments were performed at the Biomechanics Laboratory of Victoria University (Melbourne, Australia).

C. Data Processing Flow

The data processing flow is depicted in Figure 2.

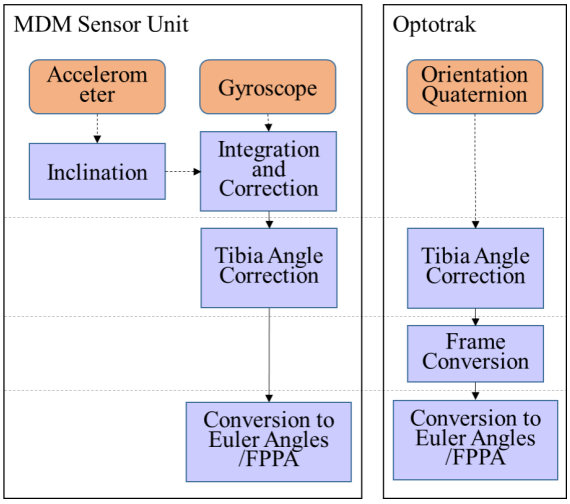

Fig. 2. Processing Flow for Sensor and Optotrak Data.

1) Processing Data from Sensor Unit: At the start of each test, initial sensor orientation is obtained using the inclination from accelerometer as the tibia segment is at rest. Orientation of the sensor (${}^{S}Q$) is then estimated by applying discrete-time integration of the gyroscope signal on the initial quaternion. This can be expressed as:

$$\alpha = \|\omega T\| \tag{1}$$

$$q_i = \left[\cos\left(\frac{\alpha}{2}\right), \sin\left(\frac{\alpha}{2}\right) \times \left[\frac{\omega T}{\|\omega T\|}\right]\right] \tag{2}$$

$${}^{S}Q_0 = {}^{S}Q_{inclination} \tag{3}$$

$${}^{S}Q_i = {}^{S}Q_{i-1} \otimes q_i, i = 1, 2, 3... \tag{4}$$

where ω is the angular velocity from gyroscope in rad/s, T is the time interval between every consecutive samples and $\otimes$ is quaternion multiplication.

The orientation ${}^{S}Q$ is then corrected using inclination from accelerometer when tibia segment is at rest (after the squat/hop). The tibia-twist angle is reset to zero at the start and end sample of the squat/hop, given the minimal tibia angular rotations in this application, and due to absence of reference to integrated gyroscope data. Linear interpolation [19] was applied to other quaternion samples to eliminate the cumulative errors caused by random walk drift from the gyroscope.

The sensor quaternion is adjusted by rotating around S_Z axis by angle θ_t (as is noted in Figure 1(b)), so that it represents orientation of tibia(${}^{T}Q$):

$${}^{T}Q = {}^{S}Q \otimes Q_{\theta_t} \tag{5}$$

where Q_{θ_t} represents the rotation quaternion caused by θ_t. Since the angle θ_t cannot be accurately measured in most practical situations, such as in a sports lab, we use an assumed value $\theta_{t,assumed}$ instead of actual θ_t.

The **3D** Euler angles (θ_x, θ_y and θ_z) of tibia can be obtained by converting the calibrated quaternion into Euler angles in XYZ sequence.

The frontal plane projection angle (FPPA) can be calculated by converting quaternion to direction cosine matrix (DCM), then applying arc-tangent function on G_X and G_Z component of the direction vector of T_Z axis:

$$FPPA = atan\left(\frac{DCM[z,x]}{DCM[z,z]}\right) \tag{6}$$

To better describe the changes of Euler angles or FPPA (θ) with respect to initial state of the tibia segment, the baseline corrected angle is calculated from Equation 7:

$$\theta_{corrected} = \theta - \theta_{baseline} \tag{7}$$

where $\theta_{baseline}$ represent the angle before squatting in squat test and that at the landing moment during the hop test, shown as the starting of grey area in Figure3(a).

2) Processing Data from Optotrak: The data obtained from Optotrak system is the quaternion that represents the orientation of the sensor, with respect from the lab-CS. Similar process is applied onto the Optotrak quaternion, following similar procedure as Equations 5 to 7. As the lab-CS axes $L_X L_Y$ are not in line with the global-CS axes $G_X G_Y$, the reference CS of the quaternion is adjusted from lab-CS to global-CS.

$${}^{G}Q_{op} = {}^{GL}Q \otimes {}^{L}Q \tag{8}$$

where ${}^{GL}Q$ is the quaternion representing rotation from lab-CS to global-CS.

Data from Optotrak is then down-sampled from 300Hz to 200Hz to match the sensor sampling frequency.

In addition, the angle θ_t is estimated by using Visual3D software [20] between sensor-CS defined by Optotrak markers, and tibia-CS found using calibration markers created at the medial and lateral aspects of the malleolus (distal shank) and femoral epicondyles (proximal shank).

D. Statistical Analysis

For comparison between sensor and reference system, Root-Mean-Square Errors (RMSEs) between baseline corrected tibia-flexion angle, tibia-adduction angle and FPPA during the period of motion are used to evaluate the accuracy of the system output. The period of motion is defined as a 2 second window during squatting in squat tests, and a 1 second window from the landing moment in hop tests. The RMSE can be expressed as Equation 9:

$$RMSE = \sqrt{\frac{\sum(\theta_{corrected,sensor} - \theta_{corrected,optotrak})^2}{N}} \tag{9}$$

where N is the number of samples in the error signal, $\theta_{corrected,sensor}$ and $\theta_{corrected,optotrak}$ represents the baseline corrected angle from sensor and Optotrak.

Moreover, we assess the effect of replacing θ_t with its assumed value $\theta_{t,assumed}$ on the overall accuracy by comparing results with different $\theta_{t,assumed}$ values ($40°$, $45°$ and $50°$).

III. Experimental Results

A. Kinematics of the Tibia Segment

Figure 3 compares examples of the tibia-flexion and tibia-adduction angles measured by the Optotrak and Inertial Sensor. The tibia-flexion angle is presented in Figure 3(a), with a range of $10° - 35°$ for the squat and hop tests period of motion (grey area in Figure 3(a)).

Figure 3(b) presents different patterns in tibia-adduction angle during simulated normal, varus and valgus motions. When the subject was performing simulated varus squats, the tibia-adduction angle is approximately 10 degrees higher than the normal squats during the period of motion (grey area

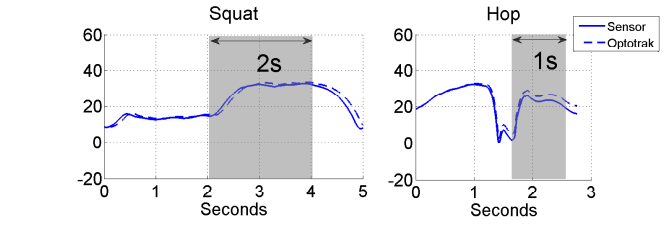

(a)

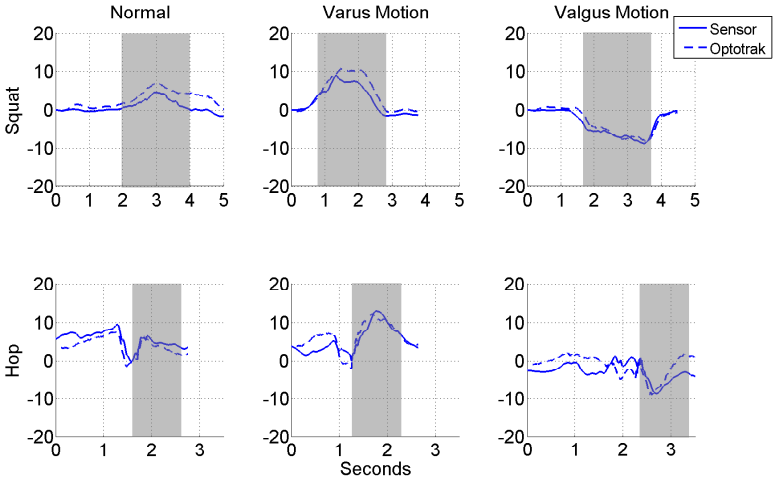

(b)

Fig. 3. Example (a) tibia-flexion angle and (b) tibia-adduction angle from squat and hop tests, compared with Optotrak. Grey area shows the period of motion.

in Figure 3(b)); while in simulated valgus squats, the tibia-adduction angle is 10 degrees lower than the normal squats during the period of motion. Similar trend can be observed in hops: the tibia-adduction angle shows positive values in simulated varus hops and negative values in simulated valgus hops.

Figure 4 compares the tibia-adduction angle and the FPPA. The FPPA has similar pattern with the tibia-adduction angle in squat (Figure 4(a)) and hop (Figure 4(b)) tests with slightly larger magnitude.

B. Analysis of Errors

The measured θ_t values are 38, 43 and 52 degrees for Subject 1, 2 and 3 respectively.

The RMSE values between the sensor and Optotrak outputs are summarized in Table I in terms of mean value and standard deviation for all subjects.

The tibia-flexion angles show low RMSE values of 1.2 ± 0.9 and 2.0 ± 1.3 degrees from the squat and hop tests respectively.

In terms of tibia-adduction angle, Subject 1's RMSE shows lowest values (1.1 ± 0.5 degrees for squat and 2.8 ± 1.6 degrees for hop) when assumed $\theta_{t,assumed} = 40°$, and highest values (2.4 ± 1.1 degrees for squat and 4.3 ± 2.5 degrees for hop) when assumed $\theta_{t,assumed} = 50°$. Similarly for Subjects 2 and 3, the RMSE shows low values when the assumed $\theta_{t,assumed}$ is close to the the measured value.

Figure 5 shows a scatter plot of RMSE of tibia-adduction angle with respect to the absolute value of the difference between $\theta_{t,assumed}$ and measured θ_t. Clear positive correlation can be seen for each subject, i.e. a higher difference between assumed and measured θ_t values leads to a larger RMSE.

The overall RMSE values of tibia-adduction angle across all subjects are 1.8 ± 1.0 and 3.3 ± 1.8 degrees from squat and hop tests respectively, with assumed $\theta_{t,assumed} = 45°$.

It has been shown in Figure 4 that the FPPA has similar pattern with the tibia-adduction angle. RMSE of the FPPA is also similar to RMSE of the tibia-adduction angle. The overall RMSE values of the FPPA are 2.3 ± 1.6 and 4.1 ± 2.3 degrees from squat and hop tests respectively, with assumed $\theta_{t,assumed} = 45°$.

IV. Discussion

The results showed good agreement between the proposed and reference systems as revealed by low RMSEs (1.6 ± 1.1 degrees on tibia-flexion angle, 2.5 ± 1.6 degrees on tibia-adduction angle and 3.2 ± 2.2 degrees on FPPA, with $\theta_{t,assumed} = 45°$).

The RMSE of tibia-adduction angle of hop tests (3.3 ± 1.8 degrees, $\theta_{t,assumed} = 45°$) was higher than that of squat tests (1.8 ± 1.0 degrees, $\theta_{t,assumed} = 45°$). When a subject is performing dynamic motions (i.e. hop and land), mechanical shock towards the tibia and knee leads to a higher skin and soft tissue artefact. This shock adversely affects the accuracy of tibia-adduction angle measurements using an inertial sensor. However, this effect can be reduced by applying compression (e.g., using an elastic band) on the sensor.

The twist-reset method used to remove gyroscope drift (Section II (C)) relies on the value of tibia-twist angle before and after a movement. If tibia-twist angle stays unchanged before and after a movement - such as, in a squat test where subjects reliably assume the same tibia position before and after squatting - the reset method is highly effective for

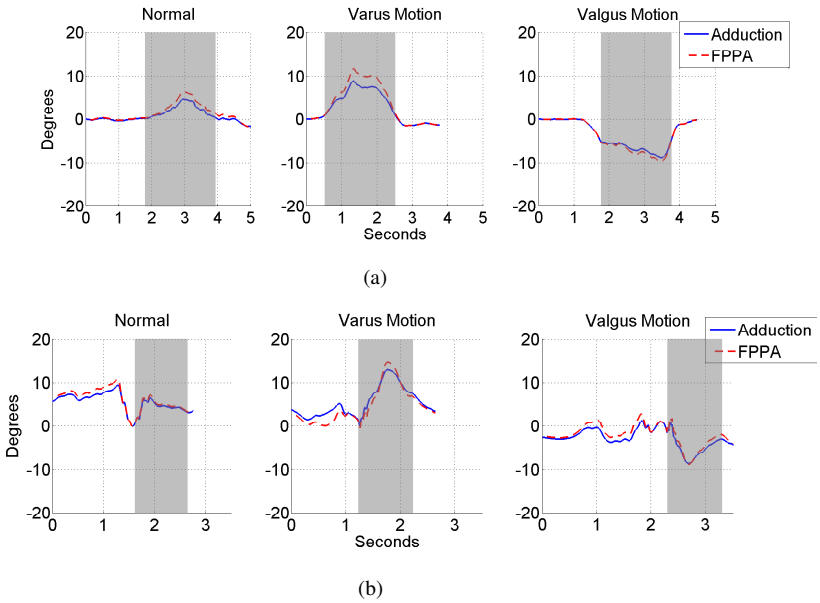

Fig. 4. Comparison between tibia-adduction angle and FPPA in example (a) squat and (b) hop tests.

removing drift. On the other hand, in dynamic movements such as single leg hopping, tibia position for most subject changes after landing and hence the twist-reset method introduces some errors. Difference in accuracy of squat and hop measurements can be partly attributed to errors arising from twist-reset method. In addition, the tibia-twist angle varies more when subjects perform simulated varus and valgus motions, leading to a larger error in these movements compared to their normal counterparts. This error can be reduced by providing careful instruction and training to the subjects. Moreover, a magnetometer can be introduced into the system to obtain a more accurate tibia-twist angle. However, the accuracy of the magnetometer is constrained by magnetic disturbances.

Some errors in the proposed system can be attributed to the difference between angle θ_t (Figure 1(c)) and its assumed value $\theta_{t,assumed}$ that we use in our processing. Results in Figure 5 show a positive correlation between the error in $\theta_{t,assumed}$ and the RMSE of tibia-adduction angle in squat and hop tests. Angle θ_t can be more accurately estimated by performing geometric measurements or careful calibration using inertial sensors.

Apart from the tibia-adduction angle, the FPPA is presented as it intuitively represents the kinematics of the knee – it corresponds to the **2D** angle taken from the frontal plane. The result indicates that varus and valgus motion can be distinguished using both the tibia-adduction angle (Figure 3(b)) and the FPPA (Figure 4(a) and 4(b)) while the FPPA has slightly larger range of motion (Figure 4).

In comparison to previous studies in knee kinematics, the proposed system uses a simplified setup with only one sensor unit attached to the tibia segment. The system does not employ any sensor unit on the femur segment, thus the skin motion effect caused by muscles and tendons on the thigh is avoided. Although the thigh angular motion is not measured, the proposed system has good performance in estimating tibia angle, which is commonly associated with knee abduction and adduction.

With excellent portability and accuracy, the system can be used to perform ambulatory measurement outside the laboratory environment, thus has great potential in on-site application in sports and rehabilitation.

Future work will study the relationship between the results from the proposed system and angular motion of both femur and tibia, improvement on accuracy of the algorithm, as well as application of the proposed system in the assessment of knee stability.

V. Conclusion

In this study, a system which employs low-power accelerometers and gyroscopes to measure tibia angular motion is proposed and the accuracy of the results is evaluated. The system provide measurements of tibia-flexion and tibia-adduction angles which showed good agreement with commercial motion capture system. This system can be further employed in knee pathologies to assess knee stability in sports players screening, performance enhancement and rehabilitation.

References

[1] J. M. Hootman, R. Dick, and J. Agel, "Epidemiology of collegiate injuries for 15 sports: summary and recommendations for injury prevention initiatives," *J Athl Train*, vol. 42, no. 2, pp. 311–319, 2007.

[2] J. G. Garrick and R. K. Requa, "ACL injuries in men and women - how common are they?" in *Prevention of Noncontact ACL Injuries*, L. Y. Griffin, Ed. Rosemont, IL: American Academy of Orthopaedic Surgeons, 2001.

[3] V. P. Kannus, "Evaluation of abnormal biomechanics of the foot and ankle in athletes," *Br J Sports Med*, vol. 26, no. 2, pp. 83–89, Jun 1992.

[4] T. E. Hewett, G. D. Myer, K. R. Ford, R. S. Heidt, A. J. Colosimo, S. G. McLean, A. J. van den Bogert, M. V. Paterno, and P. Succop, "Biomechanical measures of neuromuscular control and valgus loading of the knee predict anterior cruciate ligament injury risk in female athletes: a prospective study," *Am J Sports Med*, vol. 33, no. 4, pp. 492–501, Apr 2005.

[5] M. V. Paterno and T. E. Hewett, "Functional testing, functional training, and criteria for return to play after acl reconstruction," in *Clinical Orthopaedic Rehabilitation: An Evidence-Based Approach*, 2011, ch. 4, pp. 211–314.

[6] U. Prakash, C. A. Wigderowitz, D. W. McGurty, and D. I. Rowley, "Computerised measurement of tibiofemoral alignment," *J Bone Joint Surg Br*, vol. 83, no. 6, pp. 819–824, Aug 2001.

TABLE I. RMSE (AVERAGE±STD) OF TIBIA-FLEXION ANGLE (TF), TIBIA-ADDUCTION ANGLE (TA) AND FRONTAL PLANE PROJECTION ANGLE (FPPA) BETWEEN SENSOR AND OPTOTRAK FROM SQUAT AND HOP TESTS OF ALL SUBJECTS WITH $\theta_{t,assumed}$ VALUES 40°, 45° AND 50°

			Normal			Varus			Valgus		
$\theta_{t,assumed}$	Motion	Subject	TF RMSE	TA RMSE	FPPA RMSE	TF RMSE	TA RMSE	FPPA RMSE	TF RMSE	TA RMSE	FPPA RMSE
40°	Squat	Subject 1	1.0 ± 0.5	1.1 ± 0.5	1.2 ± 0.6	0.9 ± 0.6	1.2 ± 0.6	1.3 ± 0.6	0.7 ± 0.4	1.0 ± 0.4	1.3 ± 0.4
		Subject 2	1.4 ± 0.7	1.7 ± 0.9	2.4 ± 1.8	1.9 ± 0.7	2.1 ± 1.6	2.4 ± 0.8	2.6 ± 1.4	2.1 ± 1.0	3.2 ± 2.2
		Subject 3	0.8 ± 0.3	1.9 ± 0.9	2.0 ± 0.9	1.7 ± 0.9	2.6 ± 1.2	2.6 ± 1.1	0.6 ± 0.3	2.1 ± 1.0	2.6 ± 1.3
	Hop	Subject 1	1.5 ± 0.7	2.3 ± 1.1	2.7 ± 1.3	2.0 ± 0.7	4.0 ± 1.9	4.8 ± 2.1	1.6 ± 1.0	2.2 ± 0.8	2.7 ± 0.7
		Subject 2	1.7 ± 0.8	2.5 ± 1.1	3.4 ± 1.2	1.6 ± 1.0	2.9 ± 1.2	4.1 ± 2.1	3.3 ± 2.4	4.1 ± 2.1	5.1 ± 3.5
		Subject 3	1.3 ± 0.3	0.9 ± 0.1	0.9 ± 0.1	1.9 ± 1.1	2.5 ± 1.0	2.3 ± 1.7	3.4 ± 0.4	5.7 ± 1.5	6.4 ± 1.6
45°	Squat	Subject 1	1.0 ± 0.5	1.8 ± 1.1	2.1 ± 1.3	0.8 ± 0.6	1.5 ± 0.9	1.8 ± 1.2	0.8 ± 0.3	1.4 ± 0.2	1.6 ± 0.2
		Subject 2	1.4 ± 0.7	2.0 ± 1.6	3.4 ± 2.7	1.8 ± 0.8	2.0 ± 1.0	2.7 ± 1.5	2.4 ± 1.6	2.3 ± 1.2	3.6 ± 1.8
		Subject 3	0.8 ± 0.5	1.1 ± 0.6	1.2 ± 0.6	1.3 ± 0.8	1.9 ± 1.1	1.9 ± 1.1	0.5 ± 0.3	1.5 ± 0.8	1.8 ± 1.0
	Hop	Subject 1	1.3 ± 0.7	3.4 ± 1.5	4.0 ± 1.8	2.1 ± 0.6	4.7 ± 2.4	5.6 ± 2.7	1.3 ± 1.0	2.3 ± 0.9	2.8 ± 1.2
		Subject 2	2.2 ± 2.2	2.6 ± 1.3	3.9 ± 1.6	1.8 ± 1.0	2.9 ± 1.4	3.9 ± 1.0	2.4 ± 1.4	4.7 ± 2.0	6.7 ± 2.7
		Subject 3	1.3 ± 0.3	0.8 ± 0.1	0.9 ± 0.1	1.7 ± 1.1	2.6 ± 0.9	2.4 ± 1.6	3.2 ± 0.4	4.3 ± 1.3	4.8 ± 1.6
50°	Squat	Subject 1	1.0 ± 0.5	2.9 ± 1.4	3.5 ± 1.7	0.7 ± 0.6	2.0 ± 1.1	2.5 ± 1.6	1.0 ± 0.2	2.4 ± 0.9	2.8 ± 1.2
		Subject 2	1.2 ± 0.6	3.0 ± 2.3	5.4 ± 2.9	1.6 ± 0.9	3.0 ± 1.0	4.6 ± 2.0	2.2 ± 1.8	3.1 ± 1.7	4.3 ± 2.6
		Subject 3	0.8 ± 0.7	0.5 ± 0.2	0.6 ± 0.1	0.9 ± 0.7	1.3 ± 1.1	1.2 ± 1.1	0.4 ± 0.3	0.9 ± 0.6	1.1 ± 0.7
	Hop	Subject 1	1.3 ± 0.8	4.6 ± 2.3	5.4 ± 2.7	2.2 ± 0.5	5.4 ± 3.1	6.6 ± 3.8	4.0 ± 2.4	2.9 ± 1.3	3.4 ± 1.6
		Subject 2	2.2 ± 2.3	4.1 ± 1.7	5.7 ± 2.3	1.9 ± 0.6	3.6 ± 1.0	5.2 ± 1.6	2.0 ± 1.1	5.6 ± 2.2	8.2 ± 3.1
		Subject 3	1.3 ± 0.3	0.8 ± 0.1	1.0 ± 0.2	1.5 ± 1.2	2.6 ± 0.9	2.5 ± 1.6	2.9 ± 0.5	3.0 ± 1.0	3.4 ± 1.4

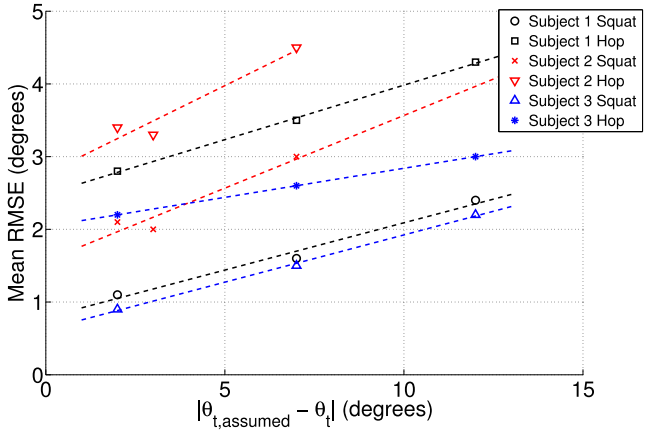

Fig. 5. Mean RMSE values of tibia-adduction angle with respect to the difference between θ_t and its assumed value $\theta_{t,assumed}$.

[7] R. L. Mizner, T. L. Chmielewski, J. J. Toepke, and K. B. Tofte, "Comparison of 2-dimensional measurement techniques for predicting knee angle and moment during a drop vertical jump," *Clin J Sport Med*, vol. 22, no. 3, pp. 221–227, May 2012.

[8] G. Cooper, I. Sheret, L. McMillan, L. McMillian, K. Siliverdis, N. Sha, D. Hodgins, L. Kenney, and D. Howard, "Inertial sensor-based knee flexion/extension angle estimation," *J Biomech*, vol. 42, no. 16, pp. 2678–2685, Dec 2009.

[9] K. Kawano, S. Kobashi, M. Yagi, K. Kondo, S. Yoshiya, and Y. Hata, "Analyzing 3d knee kinematics using accelerometers, gyroscopes and magnetometers," in *System of Systems Engineering, 2007. SoSE '07. IEEE International Conference on*, 2007, pp. 1–6.

[10] H. Dejnabadi, B. M. Jolles, and K. Aminian, "A new approach to accurate measurement of uniaxial joint angles based on a combination of accelerometers and gyroscopes," *IEEE Trans Biomed Eng*, vol. 52, no. 8, pp. 1478–1484, Aug 2005.

[11] E. Charry, W. Hu, M. Umer, A. Ronchi, and S. Taylor, "Study on estimation of peak ground reaction forces using tibial accelerations in running," in *Intelligent Sensors, Sensor Networks and Information Processing, 2013 IEEE Eighth International Conference on*, 2013, pp. 288–293.

[12] D. Paley and K. Tetsworth, "Mechanical axis deviation of the lower limbs. Preoperative planning of multiapical frontal plane angular and bowing deformities of the femur and tibia," *Clin. Orthop. Relat. Res.*, no. 280, pp. 65–71, Jul 1992.

[13] T. D. Cooke, E. A. Sled, and R. A. Scudamore, "Frontal plane knee alignment: a call for standardized measurement," *J. Rheumatol.*, vol. 34, no. 9, pp. 1796–1801, Sep 2007.

[14] dorsaVi Pty Ltd. ViPerform System. [Online]. Available: http://www.dorsavi.com/sport/viperform/

[15] LSM303DLHC data sheet. ST Microelectronics. [Online]. Available: http://www.st.com/st-web-ui/static/active/en/resource/technical/document/datasheet/DM00027543.pdf

[16] L3G4200D data sheet. ST Microelectronics. [Online]. Available: http://www.st.com/st-web-ui/static/active/en/resource/technical/document/datasheet/CD00265057.pdf

[17] N. D. Inc. Optotrak motion capture system. [Online]. Available: http://www.ndigital.com/optotrak-techspecs.php

[18] ——. First principles motion capture software. [Online]. Available: http://www.ndigital.com/lifesciences/firstprinciples.php

[19] A. M. Sabatini, C. Martelloni, S. Scapellato, and F. Cavallo, "Assessment of walking features from foot inertial sensing," *IEEE Trans Biomed Eng*, vol. 52, no. 3, pp. 486–494, Mar 2005.

[20] Visual3D 3D analysis toolkit. C-Motion Inc. [Online]. Available: http://www.c-motion.com/products/visual3d/